Optical and confocal microscopy observations of screw dislocations in smectic-*A* liquid crystals

I. Lelidis,[1] C. Blanc,[2] and M. Kléman[3]
[1]*Groupe des Cristaux Liquides, Université de Picardie, 33 rue Saint-Leu, 80039 Amiens, France*
[2]*GDPC (UMR 5581), Université de Montpellier-II, Place Eugène Bataillon, F-34095 Montpellier Cedex 05, France*
[3]*IMPMC (UMR 7590), Université Paris VI, 140 rue de Lourmel, 75915 Paris, France*
(Received 12 April 2006; revised manuscript received 5 July 2006; published 27 November 2006)

We present experimental evidence of the presence of isolated screw dislocations in smectic-*A* liquid crystals observed by polarizing microscopy. In a wedge-shaped homeotropic cell, the edge and screw dislocations interaction gives rise to a strong-enough optical contrast and makes visible their mutual intersections at temperatures close to the smectic-*A* to smectic-*C* phase transition temperature. The nature of the defects is confirmed by confocal microscopy observations. At large scale we observe a forest of screw dislocations, perpendicular to the smectic layers, across the thickness of the cell (end-on configuration). Their density varies between 10^9 and 10^{12} m^{-2}. *In situ* observations of dislocations under stress, in the optical microscope, provide quantitative information about the screw-edge dislocation interactions. The latter interaction is calculated in the unharmonic approximation and it gives rise to an observed yield stress.

DOI: 10.1103/PhysRevE.74.051710 PACS number(s): 61.30.Jf, 61.72.Ff, 61.72.Lk, 62.20.Fe

INTRODUCTION

Smectic-*A* (Sm*A*)liquid crystals are lamellar materials characterized by orientational order and one-dimensional positional order. Their layered structure gives rise to topological defects such as edge and screw dislocations, much akin to defects in solids [1,2]. Edge dislocations have been extensively studied in bulk wedge samples (so-called Grandjean-Cano wedges), where they were previously observed by polarized optical microscopy [3], and later in free standing thin films [4]. Screw dislocations have been reported in self-assembled amphiphilic systems in freeze fractured samples observed by TEM [5,6] with densities as large as 10^{12} m^{-2}, and by optical microscopy in planar oriented thermotropics under shear stress [7]. Their existence has been invoked to explain several experiments [8–12] but no direct static observation has been reported yet in thermotropic smectic liquid crystals. Based on the observations in lyotropic systems and theoretical calculations, one, however, expects that screw dislocations in thermotropic smectics should appear with large densities since their energy is rather small [1]. Nevertheless, the absence of a convenient experimental method has yet prevented from acquiring experimental data on these defects.

In the present work we report observations of screw dislocations by polarized optical microscopy. The results are retrieved by confocal microscopy observations. The density of screw dislocations is measured in various homeotropic Sm *A* samples. The optical microscope experiments reveal an interaction between screw and edge dislocations. A model is proposed in the frame of the nonlinear elasticity to described the screw–edge dislocation interaction.

EXPERIMENTS

The experimental setup is made up of a polarized-light optical microscope (Leica DMRP), an oven (Instec mK) mounted on the stage of the microscope, and a deformation micro-device, built in house, which was designed to fit the oven [13]. A couple of piezoelectric elements (Quartz & Silice) permits a compression or dilatation of the cell normal to the layers. A 3CCD camera (JVS KY-F55BE) connected to a video recorder (Panasonic SVHS) is used for image acquisition. A confocal microscope (Olympus BH2-UMA) has also been used to acquire images of thin optical sections ($\delta z \approx 0.5$ μm) into the bulk of the samples.

The liquid crystal compound is a fluorinated octyloxyphenyl octyloxybenzoate (BDH173, Fig. 1), that undergoes the following transitions: Crystal $\rightarrow$ Sm*A* at 56 °C, Sm*A* $\rightarrow$ Sm*C* (smectic-*C*) at 55 °C when cooling (monotropic), and Sm*A*-Isotropic at 79 °C. The smectic layer thickness *a* is $\simeq$3.2 nm [14]. A typical sample is composed by two optically flat glass plates in a wedge geometry. The plates are treated with the surfactant *n*,*n*-dimethyl-*n*-octadecyl-3-aminopropyltrimethoxysilyl-chloride (DMOAP, CH3-(CH2)17(Me)2N+(CH2)3Si(OMe)3Cl–, where Me denotes methyl, Fig. 1) to orient the liquid crystal molecules with their long axis perpendicular to the plate surface (homeotropic anchoring), i.e., the smectic ordering appears with layers parallel to the substrate [15].

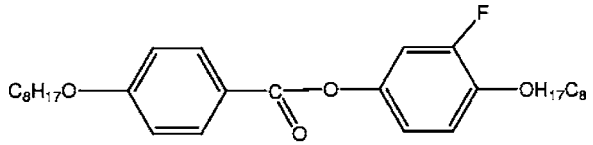

BDH173

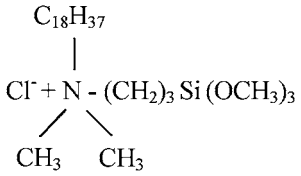

DMOAP

FIG. 1. Molecular structures of the BDH173 liquid crystal compound and the surfactant DMOAP.

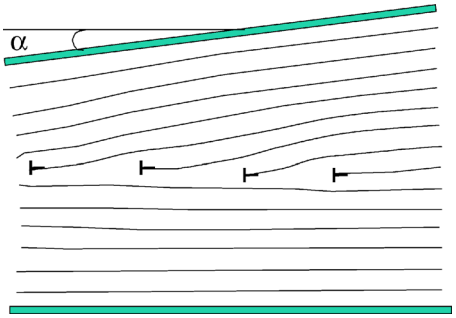

FIG. 2. (Color online) Schematic cross section of a wedge-shaped homeotropic smectic-*A* sample, containing a tilt subboundary of edge dislocations. α is the wedge angle formed by the glass plates.

The sample is mounted in the oven. The liquid crystal is introduced between the plates by capillarity in the isotropic phase. In the Sm*A* phase the wedge geometry gives rise to a tilt subboundary [3], located in the middle plane of the sample, due to the image forces [16,17]. The subboundary is made up of edge dislocations, that form a regular one-dimensional array parallel to the edge of the dihedron (Fig. 2). These edge dislocations become visible, when cooling toward the Sm*A*-Sm*C* phase transition temperature (T_{AC}), since the transition starts locally in the stress field of the defects. This happens because the strains associated with a single dislocation alter the transition temperature. A compressive stress normal to the layers raises the transition temperature and so favors the Sm*C* phase (the rodlike molecular axis is tilted by a polar angle θ with respect to the layer normal) while a tensile stress lowers it and therefore favors the Sm*A* phase. The contrast is further enhanced when the sample is observed either with slightly uncrossed polarizers or under conical incidence of light. The array period ℓ is measured directly on the microscope stage while the Burgers vector $b=na$ equals the product of ℓ times the wedge-angle α measured by Fabry-Perot interferometry and fixed in the range $\sim 10^{-4}-10^{-3}$ rad. For such low dihedral angles we always observe elementary edge dislocations ($n=1$) [18,19].

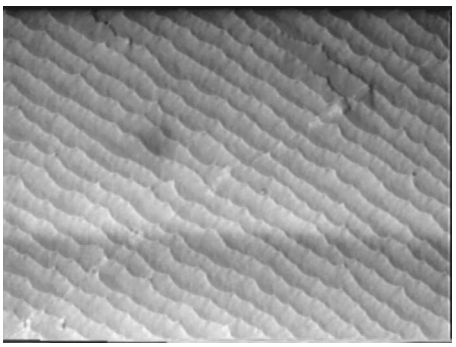

FIG. 3. Typical array of edge dislocations in a wedge-shaped homeotropic sample, viewed between slightly uncrossed polarizers close to T_{AC}. The period of the dislocation array is about 10 μm. The edge dislocations are strongly pinned on screw dislocations. The horizontal dimension of the image is 245 μm.

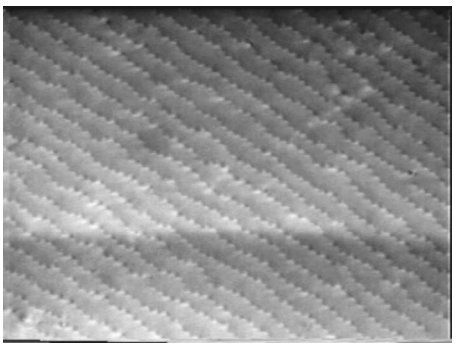

FIG. 4. The same array of edge dislocation closer to T_{AC}. A network of screw dislocations appears along the edge dislocations lines. The density of screw dislocations is 6.3×10^{10} m^{-2}. The horizontal dimension of the image is 245 μm.

Optical microscopy

Figure 3 is acquired by optical microscopy in transmission mode, under slightly uncrossed polarizers. It shows a typical aspect of the sample microstructure in the Sm*A* phase close enough to T_{AC}. As expected, an array of edge dislocations is observed parallel to the edge of the wedge. The dislocations are not straight lines but are pinned locally on dots. The distance between the dislocation lines in the array is $\ell \simeq 10$ μm, and their Burgers vector is $b=\ell\,\alpha=a$. Approaching further to T_{AC} by cooling the sample, a network of dots appears (see Fig. 4) along the edge dislocation lines. As the transition toward the Sm*C* phase proceeds, the contrast of the edge dislocation lines starts to faint while the network of the dots is still well perceivable (see Fig. 5). A few mK lower, the mechanism of contrast disappears and the dots are no longer visible. When the edge dislocations are not observable, e.g., far from the transition or for thick samples, the network of dots has never been observed.

In order to identify the origin of the observed forest of dots, we first test if the dots are fixed or not by performing *compression experiments* (in order to avoid any interference with the undulation instability [20]). In smectics, climb motion is somewhat easier than glide [21]. Under an applied compressive stress along the layer normal, the edge disloca-

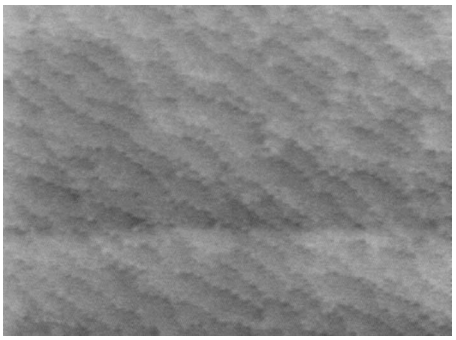

FIG. 5. Around the Sm*A*-Sm*C* transition only the screw dislocations are directly visible. Their density is 6.2×10^{10} m^{-2}. The wavy appearance of the screw dislocation network is due to the thermally activated jerky climb [24] of edge dislocations lines. The horizontal dimension of the image is 245 μm.

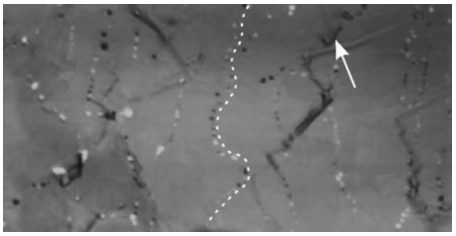

FIG. 6. Typical image of the microstructure of a Sm*A* sample acquired by confocal microscopy. The image is a stack of several images recorded along the z axis. Black and white dots correspond to screw dislocation perpendicular to the smectic layers. The mean distance of screw dislocations is 0.9 μm corresponding to a density of 1.2×10^{12} m^{-2}. The vertical dimension of the image is 23 μm.

tions experience a Peach-Koehler force parallel to the layers [22,23], and the array of edge dislocations should climb toward the thicker part of the sample, to relax the stress. Experimentally, for small-enough deformations the edge dislocations are observed to bow between the forest of dots while they remain pinned. The stress acting on these dislocations can be estimated from their radius of curvature [24]: $\sigma=Bb/R$. That stress gives an upper limit of a yield stress. When individual pinning takes place, in samples with low densities of pinning points, curvature is absent and the stress is estimated from the distance of the edge dislocation from its equilibrium position [25]. Above a yield strain ε_0, the motion of the edge dislocations is no more obstructed by the dots and plastic flow begins. The dots are not dragged along by the moving edge dislocations, which proves that they should be connected to the glass walls. The measured ε_0 corresponds to a yield stress: $\sigma_0=\epsilon_0/B\sim10^2$ to 10^3 Pa depending on the sample microstructure [24,25]. The measured ϵ_0 is independent of the applied strain rate and increases with the density of dots. The observed pinning reveals that the dots are at the intersection between the edge dislocations and a network of defects crossing the cell along its thickness, anchored on the glass plates. These defects interact with the edge dislocations. The measured low yield stress value, for plastic flow mediated by edge dislocations, indicates that the interaction should be weak.

Confocal microscopy

We test the above hypothesis by examining some samples in confocal microscopy. The sample is frozen by dipping the cell, with the liquid crystal (LC) in its Sm*A* phase, in liquid nitrogen. After one of the glass plates composing the cell is removed, the sample is observed by confocal microscopy. Figure 6 shows the microstructure of a typical sample in the Sm*A* phase. The image is a stack of several images recorded along the normal to the glass plates (z axis). Under confocal illumination, many dots with variable contrast are visible in (x,y) scans. When moving along the z axis, they remain visible from the lower surface to the upper surface, thus forming curves crossing the sample. Most of these lines are straight and normal to the glass plates. They appear as spots in Fig. 6 disposed along plane curves (see the dashed line, for example), which suggests the nearby presence of edge dislocations. The lines are perpendicular to the smectic layers and we identify them as screw dislocations. Note that some of these screw dislocations do not cross the sample perpendicularly and therefore appear as curves in Fig. 6 (see one of them shown by arrow). They often display sharp angles in the vicinity of the edge dislocation, which suggests the presence of a localized force acting on these long screw dislocations.

Screw dislocation density

The previously described method to observe screw dislocations using an optical microscope, enables us to deduce their density in an homeotropic sample by simply counting their intersections with the edge dislocations, i.e., from the linear separation of the screw dislocations. The obtained density ranges between $\sim10^9$ m^{-2} and 10^{12} m^{-2}. The same density is obtained by confocal microscopy observations. These values compare well with the screw dislocation density in lyotropic lamellar phases [6]. Densities higher than $\sim3\times10^{12}$ m^{-2} cannot be measured by the present method due to the resolution limit of the optical microscope. The measured high density of screw dislocations results from their low energy. Within the harmonic approximation, screw dislocations have only a core energy (no self-energy) nor do they interact among themselves [1]. Besides their low energy, the reason governing the screw dislocations density, seems to be surface corrugation originating from the glass plates and the surfactant treatment [26].

We conclude that there is now an appreciable body of evidence implying that the observed dots are intersections of edge dislocations with screw dislocations anchored on both boundary glass plates and being perpendicular to the smectic layers (end-on configuration). However, two questions remain:

Why do the intersections exhibit a contrast? Could the measured yield stress originate from the interaction between edge and screw dislocations?

A plausible origin of the observed contrast is the topological interactions between screw and edge dislocations. It was shown theoretically [27] that the core of a screw dislocation contains molecules in the nematic phase. When an edge dislocation crosses the core of a screw dislocation, the smectic order of the edge locally melts to the nematic phase, i.e., in the Sm*C* side of the edge, the molecules recover their position normal to the layer, and the optical path difference vanishes, giving rise to a strong-enough optical contrast: a diffuse black nematic island appears in a gray Sm*C* phase.

THEORY AND DISCUSSION

As mentioned above, the yield stress σ_0 required to cause unstable growth of pinned edge dislocations has been evaluated to be in the range $\sim10^2$ to 10^3 Pa, depending on the sample microstructure. An interaction between screw and edge dislocations could explain the measured values but within the linear approximation they do not interact. Let us calculate what happens in the unharmonic case.

To find explicitly the interaction force between a screw and an edge dislocation, we consider the deformation energy

density of a SmA phase, in the lowest nonlinear approximation [1], which writes as

$$w = \frac{1}{2}B\left[\nabla_z u - \frac{1}{2}(\nabla_\perp u)^2\right]^2 + \frac{1}{2}K(\Delta_\perp u)^2, \tag{1}$$

where B is the layer compression modulus, and K the splay elastic constant. The stress field carried by an isolated screw dislocation with distortion field: $u=\frac{b_s}{2\pi}\theta$, is given by [28]

$$\sigma_{ij} = B(1-\mathbf{n}\cdot\nabla\phi)(\mathbf{n}\cdot\nabla\phi)n_i n_j, \tag{2}$$

where $\mathbf{n}=\nabla\phi/|\nabla\phi|$ is the nematic director, $\phi=z-(b_s/2\pi)\theta$ is the phase variable, and θ is the polar angle. From the internal stress of a screw dislocation Eq. (2), and the Peach-Koehler formula [22]: $\mathbf{f}=(\mathbf{b}\cdot\bar{\bar{\sigma}})\times\mathbf{t}$, we calculate the interaction force between a screw dislocation with Burgers vector $\mathbf{b}_s=(0,0,b_s)$ and an edge dislocation along the y axis, $\mathbf{t_e}=(0,1,0)$, with Burgers vector $\mathbf{b_e}=(0,0,b_e)$. The resulting force in the direction $(\pm1,0,0)$ of the motion, on a point of the edge dislocation at a distance r from the screw dislocation is

$$f_x = -Bb_e\left[\frac{1}{\sqrt{1+(b_s/2\pi r)^2}} - 1\right]. \tag{3}$$

The total force F_{int}, acting from the screw dislocation on the edge dislocation, is obtained after integration of f_x over the length L of the edge dislocation:

$$F_{\text{int}} = -Bb_e\left[\frac{2\sqrt{4+\frac{L^2}{\mathfrak{b}^2+x^2}}E\left(\frac{L}{2}\sqrt{-\frac{1}{\mathfrak{b}^2+x^2}},1+\frac{\mathfrak{b}^2}{x^2}\right)}{\sqrt{4+\frac{L^2}{x^2}}\sqrt{1+\frac{4\mathfrak{b}^2}{L^2+4x^2}}\sqrt{-\frac{1}{\mathfrak{b}^2+x^2}}} - L\right]. \tag{4}$$

$\mathfrak{b}=b_s/2\pi$, $E(\phi,k)$ is the elliptic integral of the second kind, and x the distance between the two dislocations. The dependence of the interaction force on the distance between the dislocations is given in Fig. 7. As expected the interaction falls down rapidly with distance but at the cross section of the two dislocations the force has a finite value. Of course the above elastic interaction calculation breaks down for distances shorter than the layer thickness.

Finally, the edge dislocation will cross the screw dislocation, under the external stress $\sigma_{\text{ext}}=B\epsilon$ as far as $x=r_c\approx\mathfrak{b}$, where r_c is the core radius of the screw dislocation. For a typical sample with a screw dislocation density of 10^{11} m^{-2} and assuming $b_s=2a$, the calculated yield stress from (4) is $\sigma_0=0.6Bb_s/\pi\xi=4.\cdot10^2$ Pa, where ξ is the mean distance among screw dislocations. The latter stress is of the order of magnitude of the measured one for most of our samples. Figure 8 gives the yield stress as function of the density of the screw dislocations. The lower curve is calculated from Eq. (4) for $b_s=2a$ and the upper one for $b_s=4a$. Filled circles are experimental points. $b_s=2a$ seems the most probable value of the Burgers vector as shown in lyotropic liquid crystals since the breaking of the layers is avoided [5]. Therefore the elastic interaction between screw and edges dislocations is the microscopic origin of the measured yield stress values. Nevertheless, supplementary contributions such as elastic interactions with surface irregularities, anchoring, nucleation

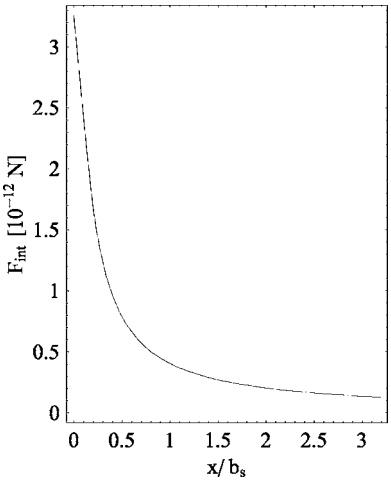

FIG. 7. Interaction force between an edge dislocation and a screw dislocation as function of their separation ($B=10^6$ J/m^3, $b_e=b_s=a$). Distance is measured in b_s units. Depinning occurs at r_c.

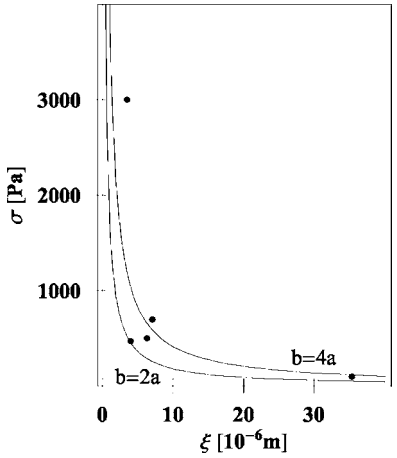

FIG. 8. Yield stress versus screw dislocation density ($b_e=a$). Curves are calculated from Eq. (4) for $b_s=2a$ lower curve and for $b_s=4a$ upper curve. Filled circles are experimental points.

of edge dislocations at the borders or inside the sample, the helical instability [29,30], etc., cannot be excluded at the present state [31] since in a few of our samples the measured yield stress is higher than the calculated one from (4).

In conclusion, we report the first observation of screw dislocations in thermotropic smectic-*A* liquid crystals by polarized optical microscopy. The method is based on the interplay of screw and edge dislocations in a homeotropic wedge-shaped sample close to the smectic-*A* to smectic-*C* phase transition temperature. Through various methods of characterization, we have evidenced a forest of screw dislocations, anchored on both boundary glass plates and perpendicular to the smectic layers. Their density ranges from 10^9 m^{-2} to 10^{12} m^{-2}. Screw dislocations interact with edge dislocations giving rise to the observed yield stress for plastic flow mediated by edge dislocations.

[1] M. Kléman, *Points. Lignes. Parois.* (Les Editions de Physique, 1977).

[2] M. Kléman and O. D. Lavrentovich, *Soft Matter Physics: An Introduction* (Springer, New York, 2003).

[3] R. B. Meyer, B. Stebler, and S. T. Lagerwall, Phys. Rev. Lett. **41**, 1393 (1978).

[4] J.-Ch. Geminard, R. Holyst, and P. Oswald, Phys. Rev. Lett. **78**, 1924 (1997).

[5] M. Kléman, C. E. Williams, M. J. Costello, and T. Gulik-Krzywicki, Philos. Mag. **35**, 33 (1977).

[6] M. Allain, Europhys. Lett. **2**, 597 (1986).

[7] C. E. Williams and M. Kléman, Philos. Mag. **33**, 213 (1976).

[8] P. Oswald and M. Kléman, J. Phys. (France) Lett. **45**, L-319 (1984).

[9] O. Dhez, F. Nallet, and O. Diat, Europhys. Lett. **55**, 821 (2001).

[10] R. A. Herke, N. A. Clark, and M. A. Handschy, Science **267**, 651 (1995).

[11] R. A. Herke, N. A. Clark, and M. A. Handschy, Phys. Rev. E **56**, 3028 (1997).

[12] S. A. Pikin, L. A. Beresnev, S. Hiller, M. Pfeiffer, and W. Haase, Mol. Mater. **3**, 1 (1993).

[13] I. Lelidis, M. Kléman, and J. L. Martin, Mol. Cryst. Liq. Cryst. Sci. Technol., Sect. A **330**, 457 (1999).

[14] Unpublished x-ray diffraction data kindly communicated by D. Tsiourvas.

[15] F. J. Kahn, Appl. Phys. Lett. **22**, 386 (1973).

[16] M. Kléman, J. Phys. (France) **35**, 595 (1974).

[17] P. S. Pershan, J. Appl. Phys. **45**, 1590 (1974).

[18] R. Bartolino and G. Durand, Mol. Cryst. Liq. Cryst. **40**, 117 (1977).

[19] F. Nallet and J. Prost, Europhys. Lett. **4**, 307 (1987).

[20] R. Ribotta, R. B. Meyer, and G. Durand, J. Phys. (France) Lett. **35**, L-161 (1974).

[21] M. Kléman and C. E. Williams, J. Phys. (France) Lett. **35**, L-49 (1974).

[22] M. Peach and J. S. Koehler, Phys. Rev. **80**, 436 (1950).

[23] J. Friedel, *Dislocations* (Pergamon, London, 1964).

[24] I. Lelidis, M. Kléman, and J. L. Martin, Mol. Cryst. Liq. Cryst. Sci. Technol., Sect. A **351**, 187 (2000).

[25] C. Blanc, N. Zuodar, I. Lelidis, M. Kléman, and J-L. Martin, Phys. Rev. E **69**, 011705 (2004).

[26] I. Lelidis and C. Öedman, Liq. Cryst. **30**, 643 (2003).

[27] S. Kralj and T. J. Sluckin, Phys. Rev. E **48**, R3244 (1993).

[28] M. Kléman and O. Parodi, J. Phys. (France) **36**, 671 (1975).

[29] J. Grilhe, Acta Metall. **11**, 57 (1963).

[30] L. Bourdon, M. Kléman, L. Lejcek, and D. Taupin, J. Phys. (France) **24**, 261 (1981).

[31] In the present analysis we do not consider the topological interaction between an edge and a screw dislocation.